Contents lists available at ScienceDirect

Physics Letters B

www.elsevier.com/locate/physletb

Probing Higgs boson couplings in H + γ production at the LHC

Hamzeh Khanpour [a,b], Sara Khatibi [b], Mojtaba Mohammadi Najafabadi [b,*]

[a] *Department of Physics, University of Science and Technology of Mazandaran, P.O.Box 48518-78195, Behshahr, Iran*
[b] *School of Particles and Accelerators, Institute for Research in Fundamental Sciences (IPM), P.O. Box 19395-5531, Tehran, Iran*

ARTICLE INFO

ABSTRACT

In this paper, we examine the potential of Higgs boson production associated with a photon at the LHC to probe the new physics effects in the framework of the standard model effective field theory. It is shown that the differential kinematic distributions such as photon transverse momentum and invariant mass of Higgs + γ in Higgs associated production are powerful variables to explore the coefficients of dimension six operators. The analysis is performed in the decay channel of Higgs boson into a $b\bar{b}$ pair including the main sources of background processes and a realistic simulation of the detector effects. We provide constraints at 95% confidence level on the Wilson coefficients of dimension-six operators affecting Higgs boson plus a photon production. We show to what extent these limits could be improved at the high luminosity LHC. The effect of these constraints on a well-motivated beyond standard model scenario is presented.

1. Introduction

After the discovery of Higgs boson by the LHC experiments [1, 2], standard model (SM) has been found to be a successful theory to describe the interactions among the fundamental particles at the electroweak scale. However, it has some shortcomings which leads us to construct new models beyond the SM. Various models such as supersymmetric SM, extra-dimensions, two-Higgs doublet models etc. have been suggested to solve the SM problems. For instance, supersymmetric extension of SM provides the possibility to stabilize the Higgs boson mass from the ultra-violet divergencies through the contributions of the supersymmetric partners of the SM particles [3]. Most of these theories lead to some modifications of the SM parameters. In particular, the Higgs boson couplings are affected by several extensions of the SM. Nevertheless, all the experimental measurements done by the LHC experiments are in agreement with the SM predictions and so far no significant deviation with respect to the SM expectations have been found [4–7]. As a result, any new degrees of freedom are expected to be well separated from the SM particles in mass [8,9]. Due to the presence of several beyond SM scenarios and in some cases similar experimental signatures, a useful way to search for new physics could be done in a model independent way. In other words, the new physics

effects could show up in the effective field theory extension of the SM which is composed of an infinite series of higher-dimensional effective operators [10–15]. It is built based on the SM degrees of freedom and its symmetries and it could be written by adding new higher than four dimension operators to the Lagrangian of the SM. The leading contribution of the SM effective Lagrangian comes from the operators of dimension-six that is based on a complete and non-redundant operator basis [16–18].

From the phenomenological point of view, these operators can affect not only the signal strengths but also the differential distributions and angular observables as they contain new vertex structures. There are many effective operators that are contributing to Higgs couplings which motivate us to look at all possible Higgs involved processes at the LHC. Studying all processes in which Higgs boson is involved such as Higgs + jets production, Higgs associated production, and processes where Higgs is off-shell is necessary to provide information of all related new couplings. So far, there have been many studies for exploring new physics effects in the Higgs boson sector at the particle colliders in the context of SM effective field theory [19–53].

At the LHC, the Higgs production mostly proceeds through gluon–gluon fusion, vector boson fusion (H + 2 jets) and associated production with a Z or a W boson. Higgs boson could also be produced associated with a pair of top or a single top quark with production rates substantially less than the gluon–gluon fusion, vector boson fusion and associated production [54]. In addition to these processes, Higgs boson can be produced in association with a

* Corresponding author.
E-mail address: mojtaba.mohammadi.najafabadi@cern.ch (M. Mohammadi Najafabadi).

photon which has a tiny rate. However, studying this process is interesting as the photon in the final state is a hard photon and is a handle to suppress the background processes. Also, models beyond the SM can affect the production cross section of this process [55].

In this article, the power of associated $H + \gamma$ production and its differential distributions are used to constrain CP-conserving dimension-six operators. Particularly, the photon transverse momentum and the invariant mass of $H + \gamma$ system are utilized to probe the new couplings effects. These observables receive significant contributions from the dimension-six operators at large values, as these effective operators lead to high momentum transfers in associated Higgs production. We will show this channel would provide useful information on Higgs boson couplings and is worth to be looked for by the LHC experiments.

In section 2, we introduce the dimension-six operators which affect Higgs boson sector. Section 3 is dedicated to discuss the production of Higgs boson in association with a photon in proton–proton collisions at the LHC. Detailed description of event generation, simulation of detector effects, selection of events and the analysis strategy are given in Section 4. The estimates of the sensitivity that could be achieved at the LHC for the considered operators are presented in section 5. The constraints are obtained using the photon transverse momentum distribution. Section 6 summarizes our conclusions.

2. Theoretical framework

In the framework of SM effective field theory, the effects of new physics are anticipated to show up as new interactions among the SM fields. These new interactions are suppressed by the inverse powers of Λ which is the characteristic scale of new physics. In this approach, all heavy new degrees of freedom are integrated out. Respecting the SM gauge symmetries, Lorentz invariance and lepton and baryon number conservation, these effects are parameterized by higher dimension operators with not-known Wilson coefficients. The dominant contributions to the observable at the LHC are coming from dimension-six operators. As a result, the Lagrangian of the SM effective theory can be written as following [10–12]:

$$L_{eff} = L_{SM} + \sum_i \frac{c_i O_i}{\Lambda^2}. \tag{1}$$

The dimension-six operators could be classified and represented in a convenient form by choosing a basis of independent dimension-six operators O_i. In this work, our focus is on the operators which are relevant to Higgs + γ process according to the strongly interacting light Higgs (SILH) basis. The SILH Lagrangian, $\mathcal{L}_{SILH}$, has the following form [56–59]:

$$\mathcal{L}_{SILH} = \frac{g_s^2 \, \bar{c}_g}{m_W^2} \Phi^\dagger \Phi G_{\mu\nu}^a G_a^{\mu\nu} + \frac{g'^2 \, \bar{c}_\gamma}{m_W^2} \Phi^\dagger \Phi B_{\mu\nu} B^{\mu\nu}$$

$$+ \frac{ig' \, \bar{c}_B}{2m_W^2} [\Phi^\dagger \overleftrightarrow{D}^\mu \Phi] \partial^\nu B_{\mu\nu} + \frac{ig \, \bar{c}_W}{2m_W^2} [\Phi^\dagger \sigma_k \overleftrightarrow{D}^\mu \Phi] D^\nu W_{\mu\nu}^k$$

$$+ \frac{ig \, \bar{c}_{HW}}{m_W^2} [D^\mu \Phi^\dagger \sigma_k D^\nu \Phi] W_{\mu\nu}^k - \frac{\bar{c}_6 \lambda}{v^2} [\Phi^\dagger \Phi]^3$$

$$+ \frac{ig' \, \bar{c}_{HB}}{m_W^2} [D^\mu \Phi^\dagger D^\nu \Phi] B_{\mu\nu} + \frac{\bar{c}_H}{2v^2} \partial^\mu [\Phi^\dagger \Phi] \partial_\mu [\Phi^\dagger \Phi]$$

$$+ \frac{\bar{c}_T}{2v^2} [\Phi^\dagger \overleftrightarrow{D}^\mu \Phi][\Phi^\dagger \overleftrightarrow{D}_\mu \Phi] - \left[\frac{\bar{c}_l}{v^2} y_\ell \, \Phi^\dagger \Phi \, \Phi \bar{L}_L e_R \right.$$

$$\left. + \frac{\bar{c}_u}{v^2} y_u \Phi^\dagger \Phi \, \Phi^\dagger \cdot \bar{Q}_L u_R + \frac{\bar{c}_d}{v^2} y_d \Phi^\dagger \Phi \, \Phi \bar{Q}_L d_R + \text{h.c.} \right], \tag{2}$$

Table 1
The relations between the anomalous Higgs boson couplings in the mass and gauge bases. a_H denotes the SM contribution of Higgs boson couplings to two photons at loop level.

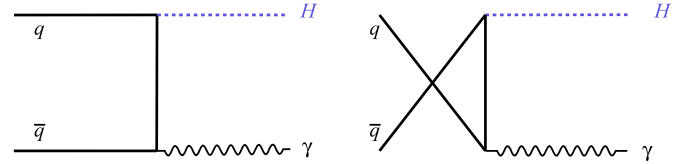| Mass basis	Gauge basis
$g_{h\gamma\gamma}$	$a_H - \frac{8gs_W^2}{m_W} \bar{c}_\gamma$
$g_{h\gamma z}^{(1)}$	$\frac{gs_W}{c_W m_W} (\bar{c}_{HW} - \bar{c}_{HB} + 8s_W^2 \bar{c}_\gamma)$
$g_{h\gamma z}^{(2)}$	$\frac{gs_W}{c_W m_W} (\bar{c}_{HW} - \bar{c}_{HB} - \bar{c}_B + \bar{c}_W)$
$\tilde{y}_u$	$y_u [1 - \frac{1}{2}\bar{c}_H + \frac{3}{2}\bar{c}_u]$
$\tilde{y}_d$	$y_d [1 - \frac{1}{2}\bar{c}_H + \frac{3}{2}\bar{c}_d]$
$g_{h\gamma uu}^{(\partial)}$	$\frac{\sqrt{2}gs_W}{m_W^2} y_u [\bar{c}_{uB} + \bar{c}_{uW}]$
$g_{h\gamma dd}^{(\partial)}$	$\frac{\sqrt{2}gs_W}{m_W^2} y_d [\bar{c}_{dB} - \bar{c}_{dW}]$

Fig. 1. Representative Feynman diagrams for Higgs + γ production in the SM at leading order.

where $B^{\mu\nu}$, $W^{\mu\nu}$, $G^{\mu\nu}$ are the electroweak and strong field strength tensors and Φ is a weak doublet which contains the Higgs boson field. In the above Lagrangian, $\Phi^\dagger \overleftrightarrow{D}^\mu \Phi = \Phi^\dagger (D^\mu \Phi) - (D^\mu \Phi)^\dagger \Phi$ and the Higgs boson is considered as a CP-even particle.

Very precisely measured oblique parameters T and S from the electroweak precision measurements reduce the number of free parameters in the SILH Lagrangian. In particular, the per-mille bounds on T and S parameters strongly constrain $\bar{c}_T$ and $\bar{c}_B + \bar{c}_W$ as they are directly related to T and S parameters [25,58–60]. In Ref. [25], constraints at 95% confidence level (CL) on the coefficients of dimension six operators have been obtained using a global fit to the LEP and the LHC Run I measurements.

This effective Lagrangian is written in gauge basis and after the electroweak symmetry breaking, it can be expressed in the mass basis. In the mass basis, the relevant subset of the Higgs boson CP-conserving anomalous couplings in unitary gauge includes [18]:

$$\mathcal{L} = -\frac{1}{4} g_{h\gamma\gamma} F_{\mu\nu} F^{\mu\nu} h - \frac{1}{2} g_{h\gamma z}^{(1)} Z_{\mu\nu} F^{\mu\nu} h - g_{h\gamma z}^{(2)} Z_\nu \partial_\mu F^{\mu\nu} h$$

$$- (\frac{\tilde{y}_u}{\sqrt{2}} [\bar{u} P_R u] h + \frac{\tilde{y}_d}{\sqrt{2}} [\bar{d} P_R d] h)$$

$$+ g_{h\gamma uu}^{(\partial)} [\bar{u} \gamma^{\mu\nu} P_R u] F_{\mu\nu} h + g_{h\gamma dd}^{(\partial)} [\bar{d} \gamma^{\mu\nu} P_R d] F_{\mu\nu} h + \text{h.c.}), \tag{3}$$

where photon and Z-boson field strength tensors denote with $F_{\mu\nu}$ and $Z_{\mu\nu}$, respectively. Table 1 presents the relations between the couplings in Eq. (3) and the Wilson coefficients in SILH Lagrangian (Eq. (2)). The SM loop induced contribution to the Higgs boson coupling to two photons ($H\gamma\gamma$) is denoted by a_H.

3. Higgs boson production in association with a photon at the LHC

In this section, we discuss the production of a Higgs boson in association with a photon in proton–proton collisions at the LHC. In the SM, at leading order, the $H + \gamma$ production proceeds through the quark–antiquark annihilation. The representative Feynman diagrams are depicted in Fig. 1.
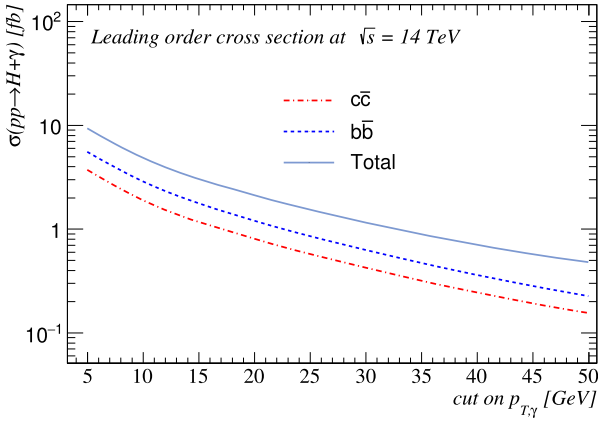
Fig. 2. Figure shows the cross section for production of H+γ at leading order versus the lower cut on photon transverse momentum at the LHC with the center-of-mass energy of 14 TeV. The contributions from $b\bar{b}$, $c\bar{c}$ annihilations are depicted separately.

The analytical expression for the differential cross section of the partonic process $q\bar{q} \to H + \gamma$ within the SM framework is given by [55]:

$$\frac{d\hat{\sigma}}{d\hat{t}} = \frac{\alpha_{em} Q_q^2 \lambda_q^2}{12}$$
$$\times \left[\frac{\hat{t}\hat{u}(1 + r_H^2) + 8r_q^2(\hat{t} + \hat{u})^2 - 2r_q(4\hat{t}\hat{u} + r_H(\hat{t} + \hat{u})^2)}{(1 - 4r_q) \times \hat{t}^2\hat{u}^2} \right], \quad (4)$$

where

$$\hat{t} = (p_b - p_\gamma)^2 - m_b^2, \ \hat{u} = (p_{\bar{b}} - p_\gamma)^2 - m_b^2,$$
$$r_H = \frac{m_H^2}{s}, \ r_q = \frac{m_q^2}{s}, \quad (5)$$

$s = (p_b + p_{\bar{b}})^2$, the quark electric charge is denoted by Q_q, and $\lambda_q = \frac{m_q}{v}$ is the Yukawa coupling of quark q. As it can be seen in Eq. (4), the presence of the electromagnetic coupling constant α_{em} and the Yukawa couplings of all light flavor quarks are suppressing factors in the production cross section of Higgs boson in association with a photon. The main source of tree level contributions come from $c\bar{c}$ and $b\bar{b}$ annihilation because of their larger Yukawa couplings. However, the contributions of $c\bar{c}$ and $b\bar{b}$ are suppressed by parton distribution function effects with respect to the lighter quarks. For more illustration, we show the production cross section of Higgs boson in association with a photon in terms of the lower cut on photon transverse momentum in Fig. 2. The contributions from $b\bar{b}$, $c\bar{c}$ annihilations are depicted separately.

At next-to-leading order, the production of $H + \gamma$ through gluon–gluon fusion is forbidden using the Furry's theorem because of the C parity conservation. The Higgs boson in association with a photon could be also produced at next-to-leading order via quark–antiquark annihilation [61]. These processes occur through box and triangle diagrams in which W, Z, Higgs, and quarks are in the loop. The cross sections of these processes are found to be smaller than the leading-order quark–antiquark annihilation so we neglect them in the present work.

Within the SM effective field theory, in addition to new diagrams, the SM diagrams are modified as well. The representative Feynman diagrams for $H + \gamma$ production are depicted in Fig. 3. The vertices which receive contributions from the SM effective field theory are shown by filled circles. As it can be seen, in addition to the SM tree level diagrams, additional diagrams depicted in the bottom of Fig. 3 contribute to the Higgs boson plus a photon at the LHC.
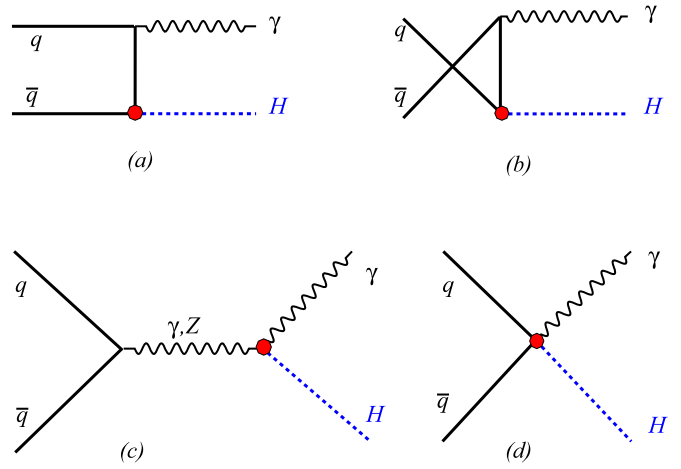

Fig. 3. Representative Feynman diagrams at tree-level for production of a Higgs boson in association with a photon at the LHC in the presence of dimension six operators.
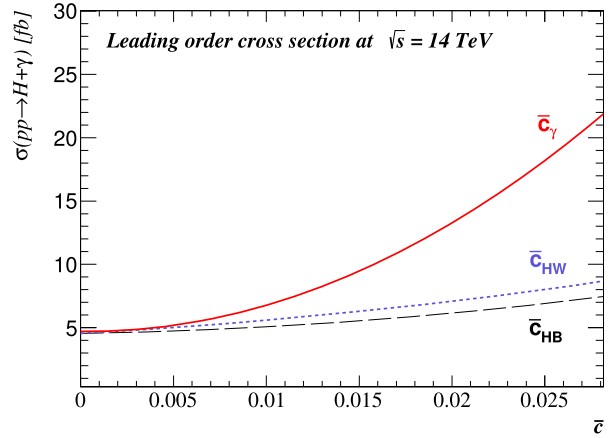

Fig. 4. The leading order cross section for production of H+γ versus the coefficients $\bar{c}_\gamma$, $\bar{c}_{HB}$, and $\bar{c}_{HW}$ at the LHC with the center-of-mass energy of 14 TeV is shown. A lower cut of 10 GeV on the photon transverse momentum has been applied.

Considering the SM effective Lagrangian, the process $pp \to H + \gamma$ is sensitive to $\bar{c}_\gamma$, $\bar{c}_{HW}$, $\bar{c}_W$, $\bar{c}_B$, $\bar{c}_{HB}$, $\bar{c}_H$, $\bar{c}_u$, $\bar{c}_d$, $\bar{c}_{uW}$, $\bar{c}_{dW}$, $\bar{c}_{uB}$, $\bar{c}_{dB}$ parameters in gauge basis and to $g_{h\gamma\gamma}$, $g_{h\gamma z}^{(1)}$, $g_{h\gamma z}^{(2)}$, $\tilde{y}_u$, $\tilde{y}_d$, $g_{h\gamma uu}^{(\partial)}$, $g_{h\gamma dd}^{(\partial)}$ couplings in the mass basis. As shown in Table 1, the latter four couplings are proportional to the Yukawa couplings of the quarks which are small for the light quarks. Therefore, the sub-processes shown in Fig. 3 (a), (b), (d) do not lead to any significant modifications in the $H + \gamma$ production cross section and are not taken into account in this analysis. As a consequence, we concentrate only on the remaining four parameters: $\bar{c}_\gamma$, $\bar{c}_{HW}$, $\bar{c}_W$, and $\bar{c}_{HB}$.

Fig. 4 shows the production cross section of H + γ in terms of the Wilson coefficients $\bar{c}_\gamma$, $\bar{c}_{HB}$, and $\bar{c}_{HW}$. To calculate the cross sections, a lower cut of 10 GeV has been set on the photon transverse momentum. As it can be seen, there is a significant sensitivity to $\bar{c}_\gamma$ while $\bar{c}_{HB}$ and $\bar{c}_{HW}$ have smaller effects on the production rate. It should be mentioned that $\bar{c}_W$ and $\bar{c}_B$ are found to have no big effect in the cross section.

In this work, the effects of the dimension six operators on $H + \gamma$ production are calculated at the LHC using Mad-Graph5-aMC@NLO [62,63]. The effective SM Lagrangian presented in Eq. (2) has been implemented in FeynRule program [64] and then the UFO model [65] is inserted into MadGraph5-aMC@NLO.
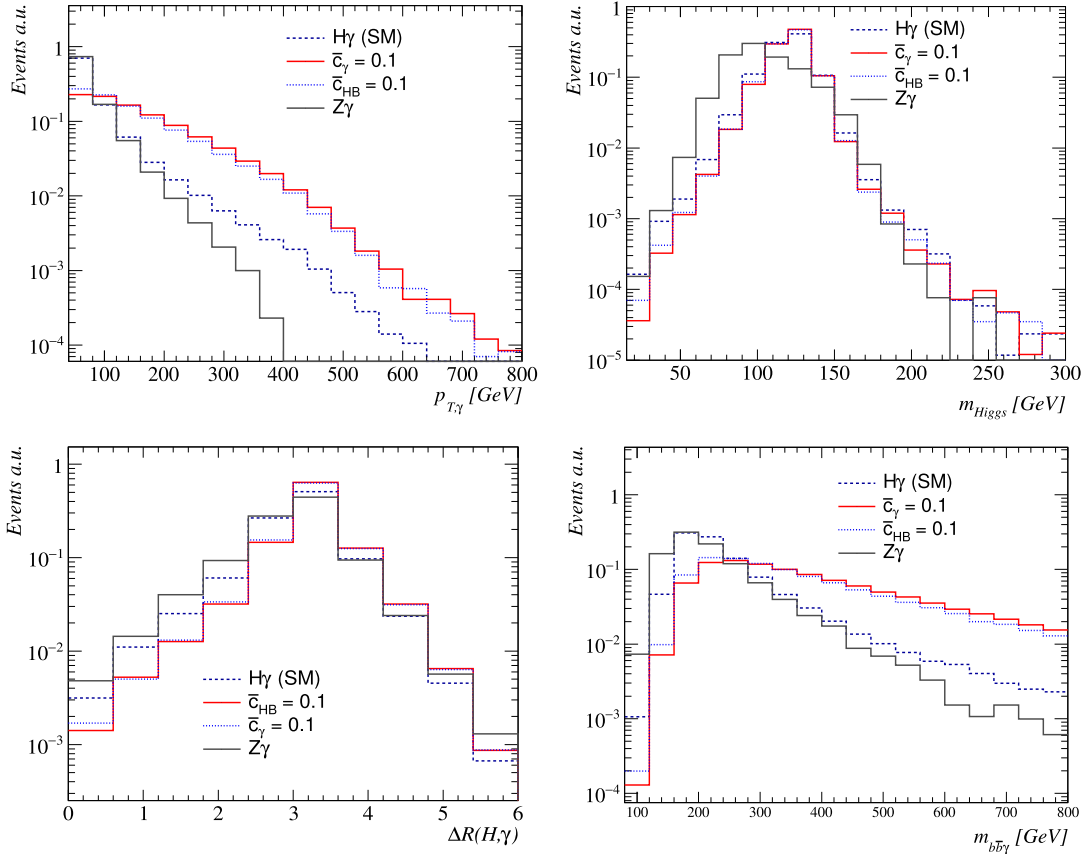
Fig. 5. Plots show the transverse momentum of the photon (upper left), the mass of reconstructed Higgs boson (upper right), the $\Delta R(H, \gamma)$ (lower left), and the invariant mass of the $H + \gamma$ system (lower right) for the SM $H + \gamma$, effective SM with $\bar{c}_\gamma = 0.1$ and $\bar{c}_{HB} = 0.1$ and $Z\gamma$ background process. (For interpretation of the references to color in this figure legend, the reader is referred to the web version of this article.)

The details could be found in Refs. [18]. We will discuss the details of simulations and determination of the 95% CL constraints on the coefficients of dimension six operators in the next section.

4. Simulation details and analysis strategy

In this section, we present the simulation details and the analysis strategy for exploring the effective SM in Higgs boson production associated with a photon. Due to large branching fraction, we consider the Higgs boson decay into a pair of bottom quarks. Consequently, the final state consists of one energetic photon together with two jets originating from the hadronization of b-quarks.

The main sources of background processes which are taken into account in this work are $W^\pm \gamma + $ jets, $Z\gamma + $ jets, $\gamma + $ jets, top $+ \gamma + $ jets, $t\bar{t} + \gamma$. MadGraph5-aMC@NLO event generator is used to generate the effective SM signal and background processes [62,63]. We generate events at the center-of-mass energy of 14 TeV at the LHC using the NNPDF2.3 [70] set of parton distribution functions. In the event generation process, the SM input parameters are taken as [71]: $m_W = 80.385$ GeV, $m_H = 125.0$ GeV, $m_t = 173.34$ GeV and $m_Z = 91.187$ GeV. The events are passed through PYTHIA 8 [66,67] for showering of partons, hadronization, and unstable particles decays. Delphes 3.3.2 [68,69] allows to simulate a CMS-like detector effects.

Jets are reconstructed using anti-k_t algorithm [72] with a radius parameter of R = 0.5. This is performed through the FastJet package [73]. The efficiency of b-tagging and the misidentification rates are taken to be dependent on the transverse momentum of jets according to the following formulas [74]:

$$\epsilon_b(p_T) = 0.85 \times \tanh(0.0025 \times p_T) \times \left(\frac{25.0}{1 + 0.063 \times p_T}\right),$$

mis-id. rate of c-jets $= 0.25 \times \tanh(0.018 \times p_T)$

$$\times \left(\frac{1.0}{1 + 0.0013 \times p_T}\right), \tag{6}$$

mis-id. rate of light-jets $= 0.01 + 0.000038 \times p_T$.

The b-tagging efficiency for a jet with $p_T = 50$ GeV is around 64%, while the c-jet misidentification rate is 17%, and light flavor jets misidentification rate is 1.1%.

To select signal events, we require that photon has a transverse momentum p_T and pseudorapidity η satisfying $p_T > 40$ GeV and $|\eta| < 2.5$. Any event containing a charged lepton with $p_T > 10$ GeV and $|\eta| < 2.5$ or missing transverse energy above 30 GeV is vetoed. Events are selected by demanding the presence of two b-jets with $p_T > 20$ GeV and $|\eta| < 2.5$. To ensure all selected objects are well-isolated, the angular separation $\Delta R(\gamma, b - \text{jets}) = \sqrt{(\Delta\phi)^2 + (\Delta\eta)^2} > 0.4$ and $\Delta R(b_1, b_2) > 0.4$. The above described selection are denoted as preselection cuts.

In Fig. 5, we present the transverse momentum of the photon (upper left), mass of the reconstructed Higgs boson from $b\bar{b}$ pair (upper right), the $\Delta R(H, \gamma)$ (lower left), and the invariant mass of the $H + \gamma$ system (lower right) for the irreducible SM background process $Z\gamma$, SM $H + \gamma$, and for effective SM with $\bar{c}_\gamma = 0.1$ and $\bar{c}_{HB} = 0.1$. All these distributions are depicted after applying the so called preselection cuts described previously.

From the photon transverse momentum spectrum and invariant mass of the $H + \gamma$ system, one can see that due to the presence of derivatives in the induced couplings of the effective SM, significant

Table 2

Expected cross sections in unit of fb after different combinations of cuts for signal and SM background processes. The signal cross sections are corresponding to particular values of $\bar{c}_\gamma = 0.1$, $\bar{c}_{HB} = 0.1$. More details of the cuts are given in the text.

$\sqrt{s} = 14$ TeV	Signal		Background processes			
Cuts	$\bar{c}_\gamma$	$\bar{c}_{HB}$	γ + jets	$tj\gamma + t\bar{t}\gamma$	$W\gamma + Z\gamma$	SM (Hγ)
One photon and lepton veto	126.3	20.99	4.443×10^6	164.92	10286.4	0.450
Only 2 b-jets, $\Delta R_{i,j} > 0.4; i, j = \gamma, b$	19.77	3.41	13026.2	0.0312	119.57	0.080
$90 < m_{b\bar{b}} < 160$ GeV and $\Delta R(H, \gamma) > 2.4$	17.88	3.06	6397.6	0.0165	58.41	0.067
$m_{b\bar{b}\gamma} > 250$ and $p_T^\gamma > 400$ GeV	0.51	0.076	0.0	0.0	0.0	0.0003

enhancements in the tail of photon p_T and $m_{H\gamma}$ appear. This is a specific feature of new effective interactions which allows us to differentiate between new physics and SM background processes.

For further reduction of the SM background contributions additional cuts are applied. A window cut on the reconstructed Higgs boson mass leads to suppress backgrounds without a Higgs boson in the final state. Thus, it is required that $90 < m_{b\bar{b}} < 160$ GeV. The angular separation between the reconstructed Higgs boson and photon candidate is required to be greater than 2.4 which is useful to suppress the γ + jets background process. A cut on the invariant mass of H + γ reduces the contribution of all background processes.

Cross sections of signal for the cases of $\bar{c}_\gamma = 0.1$, $\bar{c}_{HB} = 0.1$ and background processes after applying each set of cuts are shown in Table 2. The cross sections are given in the unit of fb. Since the background contributions overwhelm the signal in the lower values of cut on photon transverse momentum, we concentrate on the region where the signal-to-background ratio is large enough to determine the exclusion limits.

At the end of this section, a discussion is given on the potential contribution of background coming from multijet production where jets are misidentified as photons. Such a signature could come up when in the jet fragmentation, neutral pions appear and decay into two photons with a large boost. As a result, the two photon showers will overlap in the electromagnetic calorimeter and will not be separately distinguishable and they appear as a single photon in the detector. The ability for rejecting jets faking photons is crucial to suppress the QCD multijet background which has several orders of magnitude larger cross section with respect to the other background processes. After the kinematic requirements (except those related to photon) in our analysis as well as the requirement of the presence of only two b-jets, the cross section of multijet background reduces to around 10^3 pb. The jet fake photon probability varies with the fake photon transverse momentum and is at the order of $10^{-5,-4}$ for the high p_T fake photons ($p_T > 200$ GeV). Consequently, the requirement of a photon with large transverse momentum decreases the contribution of this background to a negligible level. We neglect this background in this analysis nevertheless a dedicated and more realistic detector simulation must be performed in order to estimate possible contribution of this background.

5. Results and interpretation

In this section, we present the potential sensitivities of the Higgs boson production in association with a photon to the dimension-six operators. The main coefficients affecting the Higgs + γ production that are our interest in this analysis are $\bar{c}_\gamma$, $\bar{c}_{HW}$, and $\bar{c}_{HB}$. Constraints derivation is based on the fact that dimension-six operators generate a higher tail at the large values of photon transverse momentum. As a result, we make use of the tail of photon transverse momentum, where the contribution of the SM background processes are negligible, to obtain the limits on the relevant dimension-six operators. As the number of

Table 3

Predicted constraints at 95% CL on dimension-six operator coefficients for the LHC with 14 TeV with the integrated luminosities of 300 fb^{-1} and 3000 fb^{-1}. At a time one of the couplings is considered in the analysis.

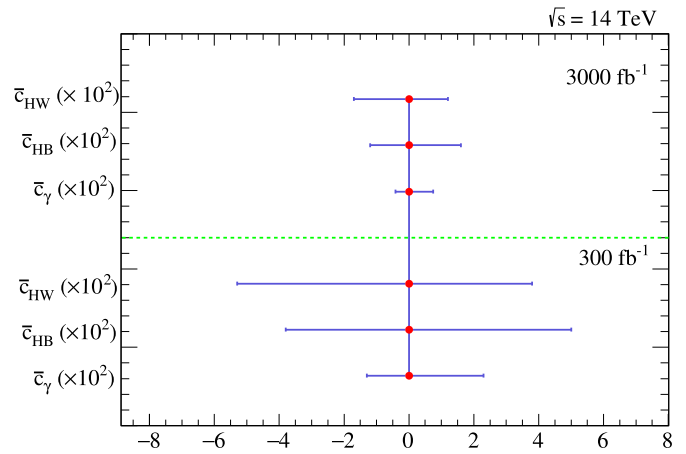| Coefficient	$\mathcal{L} = 300$ fb^{-1}	$\mathcal{L} = 3000$ fb^{-1}
$\bar{c}_\gamma$	[−0.013, 0.023]	[−0.0042, 0.0075]
$\bar{c}_{HB}$	[−0.038, 0.050]	[−0.012, 0.016]
$\bar{c}_{HW}$	[−0.053, 0.038]	[−0.017, 0.012]

Fig. 6. The 95% CL ranges obtained in a fit to the dimension-six operator coefficients individually (setting the others to zero). The results are presented for the integrated luminosities of 300 fb^{-1} and 3 ab^{-1}.

signal events increases quickly with the $\bar{c}_\gamma$, $\bar{c}_{HW}$, and $\bar{c}_{HB}$ in the tail of $p_{T,\gamma}$ and the background contribution is significantly suppressed, a χ^2 fit is performed in this region to get the 95% CL ranges. To obtain the predicted limits, only one coefficient is considered in the fit. The predicted bounds at 95% CL for the LHC at $\sqrt{s} = 14$ TeV with an integrated luminosity of 300 fb^{-1} and 3000 fb^{-1} are presented in Table 3. To obtain the results, only statistical uncertainties are considered and the effects of systematic and theoretical sources are neglected. The results are also depicted in Fig. 6 for the integrated luminosities of 300 and 3000 fb^{-1}. As it can be seen, the most sensitivity is to $\bar{c}_\gamma$ which is expected to be probed down to 10^{-3} while $\bar{c}_{HB}$ and $\bar{c}_{HW}$ are potentially explored at the order of 10^{-2} at the 95% CL.

At this point it should be mentioned that based on Fig. 5 (lower right), the information from the tail of the invariant mass distribution of H + γ could also be used to extract the constraints on the coefficients. As it can be seen, while the expectation of the SM steeply drops for the invariant mass values larger than around 300 GeV, the new physics effects shows a tail extending up to around the TeV scale. However, in a realistic analysis, more systematic uncertainties with respect to the photon transverse momentum distribution enters in the analysis using $m_{H\gamma}$ differential distribution.

It is informative to compare the results obtained in this study with the expected bounds at high luminosity LHC with other channels. In Ref. [75], considering the production modes $pp \to H + j$, $pp \to H + 2j$, $pp \to H$, $pp \to W + H$, $pp \to Z + H$, and $pp \to t\bar{t} + H$, constraints are set on the dimension-six operator coefficients. The following bounds have been obtained on $\bar{c}_\gamma, \bar{c}_{HW}, \bar{c}_{HB}$ at 95% CL at the center-of-mass energy of 14 TeV with 3000 fb^{-1} based on the expected signal strength:

$$-0.027 < \bar{c}_{HW} < 0.028, \quad -0.026 < \bar{c}_{HB} < 0.027,$$
$$-0.00029 < \bar{c}_\gamma < 0.00027. \tag{7}$$

The limits on $\bar{c}_{HW}$ and $\bar{c}_{HB}$ are the same order of the ones could be achieved from this study. However, they could be improved using a shape analysis on the Higgs transverse momentum as:

$$-0.004 < \bar{c}_{HW} < 0.004, \quad -0.004 < \bar{c}_{HB} < 0.004,$$
$$-0.00016 < \bar{c}_\gamma < 0.00013. \tag{8}$$

It should be mentioned that two improvements to the limits on dimension-six coefficients would be the combination of $H + \gamma$ channel with the other channels discussed in Ref. [75] as well as considering the complete next-to-leading order predictions for the process of $H + \gamma$ with the dimension-six couplings.

As it is well-known, the effective field theory configuration provides the possibility to constrain UV models parameters. In Ref. [76], the matching of dimension-six operators with few UV models are studied. The discussed UV models are corresponding to extension of the Higgs sector of the SM with adding a scalar doublet (two-Higgs doublet models), or with a radion or a dilaton or with including an extra scalar singlet. By matching the dimension-six operators to the UV theories, one could see that an operator can be generated in these models at tree level, at one loop or at higher orders. For example, the exchange of a radion or a dilaton scalar generates $\bar{c}_\gamma, \bar{c}_{HW}, \bar{c}_{HB}, \bar{c}_H, \bar{c}_6, \bar{c}_T, \bar{c}_W, \bar{c}_B$, and $\bar{c}_g$ at tree level. A radion could arise from the excitation of graviton in extra dimensions and a dilaton come from spontaneous breaking of scale invariance. Detailed description of the models could be found in [76–78]. The coefficients of dimension-six operators are related to the radion/dilaton model parameters according to the following:

$$\bar{c}_\gamma = -\frac{b_1 \alpha_1 g^2}{4\pi g'^2} \frac{m_H^2 v^2}{f^2 m_r^2}, \quad \bar{c}_{HB} = -\frac{b_1 \alpha_1}{4} \frac{m_H^2 v^2}{f^2 m_r^2},$$
$$\bar{c}_{HW} = -\frac{b_2 \alpha_2}{4} \frac{m_H^2 v^2}{f^2 m_r^2}, \quad \bar{c}_H = \frac{8 m_H^2 v^2}{f^2 m_r^2}, \tag{9}$$

where b_i are the coefficients of β function which for dilatons violate the scale invariance anomalously and for radions are the localized fields contribution near the IR brane [76–78]. The couplings constants corresponding to the SM gauge groups $SU(3) \times SU(2) \times U(1)$ are denoted by $\alpha_{1,2,3}$. m_r and f are the dilaton/radion mass and compactification scale (spontaneous symmetry breaking scale). Fig. 7 shows the 95% CL exclusion region of the dilaton mass and the dilaton field coupling obtained from the exclusion range of $\bar{c}_\gamma$. In this plot, the parameter $x = \frac{g}{g'} \times \sqrt{b_1 \alpha_1}$. The regions are depicted for the LHC with 300 fb^{-1} and 3 ab^{-1}. We see that LHC would be able to extend the reach for the mass of radion to TeV scale (depending on the couplings and the value of f).

6. Summary and outlook

According to the recent measurements of the LHC experiments, Higgs boson properties are found to be consistent with the SM predictions within the uncertainties and so far no considerable sign of
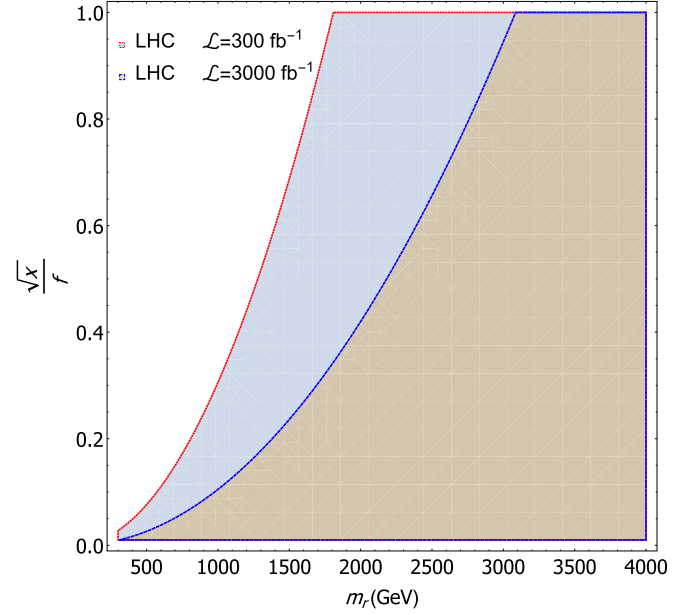

Fig. 7. The 95% CL ranges obtained on the dilaton mass and the dilaton field coupling obtained from the exclusion range of $\bar{c}_\gamma$. The parameter x is defined as $\frac{g}{g'} \times \sqrt{b_1 \alpha_1}$. (For interpretation of the references to color in this figure legend, the reader is referred to the web version of this article.)

new physics has been found. As a result, in order to search for the possible effects of new physics one can focus on the SM effective theory which relies on dimension-six operators whose contributions are suppressed by the second power of new physics scale. In the present work, we have studied the impact of dimension-six operators of the SM effective field theory related to the Higgs boson production in association with a photon at the LHC. In particular, the search is performed in the SILH basis in which a complete set of dimension-six operators with minimum assumptions on the Wilson coefficients is considered. We have restricted ourselves to the set of CP-even operators which affect the Higgs $+ \gamma$ production at tree level and concentrate only the Higgs boson decays into $b\bar{b}$ pairs. The dimension-six operators which contain derivative interactions modify the kinematics of Higgs $+ \gamma$ production. Specially, the tails of photon transverse momentum and the invariant mass of the Higgs $+ \gamma$ ($m_{H\gamma}$) receive significant contributions from the new couplings. Considering a fast detector simulation with Delphes and the main sources of background processes, stringent bounds on the coefficients of dimension-six operators have been obtained using the information of the tail of photon transverse momentum. It is found that the H $+ \gamma$ production allows us to probe $\bar{c}_\gamma$ and $\bar{c}_{HW} (\bar{c}_{HB})$ down to 10^{-3} and 10^{-2}, respectively, with an integrated luminosity of 3000 fb^{-1}.

Matching between the Wilson coefficients and UV models, we have the opportunity to probe the parameters of the UV models. In particular, we have constrained the radion/dilaton parameters and found out the mass of dilaton up to the scale of few TeV is accessible.

There are possibilities for improvement of our results listed in the following. The first way of improvement is to use the complete next-to-leading order predictions for the process of H $+ \gamma$ with the dimension-six couplings [79]. Second possibility is the incorporation of the H $+ \gamma +$ jet process [80,81] into our analysis which would increase the sensitivity. The third way of increasing the sensitivity is the inclusion of other decay modes of the Higgs boson such as WW, ZZ, etc. which allows to have more statistics and possibly leads to more stringent bounds. At the end, including the Higgs $+ \gamma$ process in a global fit with other production processes

at the LHC would affect the exclusion ranges and may improve the sensitivities.

Acknowledgements

Hamzeh Khanpour is thankful to School of Particles and Accelerators, Institute for Research in Fundamental Sciences (IPM), and University of Science and Technology of Mazandaran for financial support of this project. Sara Khatibi would like to thank Iran National Science Foundation (INSF) for the financial support.

References

[1] G. Aad, et al., ATLAS Collaboration, Phys. Lett. B 716 (2012) 1, http://dx.doi.org/10.1016/j.physletb.2012.08.020, arXiv:1207.7214 [hep-ex].

[2] S. Chatrchyan, et al., CMS Collaboration, Phys. Lett. B 716 (2012) 30, http://dx.doi.org/10.1016/j.physletb.2012.08.021, arXiv:1207.7235 [hep-ex].

[3] H.P. Nilles, Phys. Rep. 110 (1984) 1, http://dx.doi.org/10.1016/0370-1573(84)90008-5.

[4] S. Chatrchyan, et al., CMS Collaboration, J. High Energy Phys. 1306 (2013) 081, http://dx.doi.org/10.1007/JHEP06(2013)081, arXiv:1303.4571 [hep-ex].

[5] G. Aad, et al., ATLAS Collaboration, Phys. Lett. B 726 (2013) 88, http://dx.doi.org/10.1016/j.physletb.2014.05.011, arXiv:1307.1427 [hep-ex], Phys. Lett. B 734 (2014) 406, http://dx.doi.org/10.1016/j.physletb.2013.08.010 (Erratum).

[6] A. Djouadi, G. Moreau, Eur. Phys. J. C 73 (9) (2013) 2512, http://dx.doi.org/10.1140/epjc/s10052-013-2512-9, arXiv:1303.6591 [hep-ph].

[7] D. Carmi, A. Falkowski, E. Kuflik, T. Volansky, J. Zupan, J. High Energy Phys. 1210 (2012) 196, http://dx.doi.org/10.1007/JHEP10(2012)196, arXiv:1207.1718 [hep-ph].

[8] K.G. Wilson, Rev. Mod. Phys. 55 (1983) 583, http://dx.doi.org/10.1103/RevModPhys.55.583.

[9] T. Appelquist, J. Carazzone, Phys. Rev. D 11 (1975) 2856, http://dx.doi.org/10.1103/PhysRevD.11.2856.

[10] W. Buchmuller, D. Wyler, Nucl. Phys. B 268 (1986) 621, http://dx.doi.org/10.1016/0550-3213(86)90262-2.

[11] B. Grzadkowski, M. Iskrzynski, M. Misiak, J. Rosiek, J. High Energy Phys. 1010 (2010) 085, http://dx.doi.org/10.1007/JHEP10(2010)085, arXiv:1008.4884 [hep-ph].

[12] K. Hagiwara, S. Ishihara, R. Szalapski, D. Zeppenfeld, Phys. Rev. D 48 (1993) 2182, http://dx.doi.org/10.1103/PhysRevD.48.2182.

[13] C.N. Leung, S.T. Love, S. Rao, Z. Phys. C 31 (1986) 433, http://dx.doi.org/10.1007/BF01588041.

[14] M.B. Einhorn, J. Wudka, Nucl. Phys. B 876 (2013) 556, http://dx.doi.org/10.1016/j.nuclphysb.2013.08.023, arXiv:1307.0478 [hep-ph].

[15] S. Willenbrock, C. Zhang, Annu. Rev. Nucl. Part. Sci. 64 (2014) 83, http://dx.doi.org/10.1146/annurev-nucl-102313-025623, arXiv:1401.0470 [hep-ph].

[16] R. Contino, M. Ghezzi, C. Grojean, M. Muhlleitner, M. Spira, J. High Energy Phys. 1307 (2013) 035, http://dx.doi.org/10.1007/JHEP07(2013)035, arXiv:1303.3876 [hep-ph].

[17] R.S. Gupta, A. Pomarol, F. Riva, Phys. Rev. D 91 (3) (2015) 035001, http://dx.doi.org/10.1103/PhysRevD.91.035001, arXiv:1405.0181 [hep-ph].

[18] A. Alloul, B. Fuks, V. Sanz, J. High Energy Phys. 1404 (2014) 110, http://dx.doi.org/10.1007/JHEP04(2014)110, arXiv:1310.5150 [hep-ph].

[19] J.R. Espinosa, C. Grojean, M. Muhlleitner, M. Trott, J. High Energy Phys. 1212 (2012) 045, http://dx.doi.org/10.1007/JHEP12(2012)045, arXiv:1207.1717 [hep-ph].

[20] T. Corbett, O.J.P. Eboli, J. Gonzalez-Fraile, M.C. Gonzalez-Garcia, Phys. Rev. D 87 (2013) 015022, http://dx.doi.org/10.1103/PhysRevD.87.015022, arXiv:1211.4580 [hep-ph].

[21] M.E. Peskin, arXiv:1207.2516 [hep-ph].

[22] B. Dumont, S. Fichet, G. von Gersdorff, J. High Energy Phys. 1307 (2013) 065, http://dx.doi.org/10.1007/JHEP07(2013)065, arXiv:1304.3369 [hep-ph].

[23] D. Lopez-Val, T. Plehn, M. Rauch, J. High Energy Phys. 1310 (2013) 134, http://dx.doi.org/10.1007/JHEP10(2013)134, arXiv:1308.1979 [hep-ph].

[24] C. Englert, A. Freitas, M.M. Muhlleitner, T. Plehn, M. Rauch, M. Spira, K. Walz, J. Phys. G 41 (2014) 113001, http://dx.doi.org/10.1088/0954-3899/41/11/113001, arXiv:1403.7191 [hep-ph].

[25] J. Ellis, V. Sanz, T. You, J. High Energy Phys. 1503 (2015) 157, http://dx.doi.org/10.1007/JHEP03(2015)157, arXiv:1410.7703 [hep-ph].

[26] A. Falkowski, F. Riva, J. High Energy Phys. 1502 (2015) 039, http://dx.doi.org/10.1007/JHEP02(2015)039, arXiv:1411.0669 [hep-ph].

[27] T. Corbett, O.J.P. Eboli, D. Goncalves, J. Gonzalez-Fraile, T. Plehn, M. Rauch, J. High Energy Phys. 1508 (2015) 156, http://dx.doi.org/10.1007/JHEP08(2015)156, arXiv:1505.05516 [hep-ph].

[28] G. Buchalla, O. Cata, A. Celis, C. Krause, Eur. Phys. J. C 76 (5) (2016) 233, http://dx.doi.org/10.1140/epjc/s10052-016-4086-9, arXiv:1511.00988 [hep-ph].

[29] T. Plehn, M. Rauch, Europhys. Lett. 100 (2012) 11002, http://dx.doi.org/10.1209/0295-5075/100/11002, arXiv:1207.6108 [hep-ph].

[30] T. Corbett, O.J.P. Eboli, J. Gonzalez-Fraile, M.C. Gonzalez-Garcia, Phys. Rev. D 86 (2012) 075013, http://dx.doi.org/10.1103/PhysRevD.86.075013, arXiv:1207.1344 [hep-ph].

[31] J. Ellis, V. Sanz, T. You, J. High Energy Phys. 1407 (2014) 036, http://dx.doi.org/10.1007/JHEP07(2014)036, arXiv:1404.3667 [hep-ph].

[32] F. Ferreira, B. Fuks, V. Sanz, D. Sengupta, arXiv:1612.01808 [hep-ph].

[33] A. Azatov, R. Contino, J. Galloway, J. High Energy Phys. 1204 (2012) 127, http://dx.doi.org/10.1007/JHEP04(2012)127, arXiv:1202.3415 [hep-ph], J. High Energy Phys. 1304 (2013) 140, http://dx.doi.org/10.1007/JHEP04(2013)140 (Erratum).

[34] L. Berthier, M. Trott, J. High Energy Phys. 1602 (2016) 069, http://dx.doi.org/10.1007/JHEP02(2016)069, arXiv:1508.05060 [hep-ph].

[35] A. Efrati, A. Falkowski, Y. Soreq, J. High Energy Phys. 1507 (2015) 018, http://dx.doi.org/10.1007/JHEP07(2015)018, arXiv:1503.07872 [hep-ph].

[36] H. Bélusca-Maïto, A. Falkowski, D. Fontes, J.C. Romão, J.P. Silva, arXiv:1611.01112 [hep-ph].

[37] S. Bar-Shalom, A. Soni, J. Wudka, Phys. Rev. D 92 (1) (2015) 015018, http://dx.doi.org/10.1103/PhysRevD.92.015018, arXiv:1405.2924 [hep-ph].

[38] J. Cohen, S. Bar-Shalom, G. Eilam, Phys. Rev. D 94 (3) (2016) 035030, http://dx.doi.org/10.1103/PhysRevD.94.035030, arXiv:1602.01698 [hep-ph].

[39] C. Englert, Y. Soreq, M. Spannowsky, J. High Energy Phys. 1505 (2015) 145, http://dx.doi.org/10.1007/JHEP05(2015)145, arXiv:1410.5440 [hep-ph].

[40] C. Englert, M. Spannowsky, Phys. Lett. B 740 (2015) 8, http://dx.doi.org/10.1016/j.physletb.2014.11.035, arXiv:1408.5147 [hep-ph].

[41] M.J. Dolan, C. Englert, N. Greiner, K. Nordstrom, M. Spannowsky, Eur. Phys. J. C 75 (8) (2015) 387, http://dx.doi.org/10.1140/epjc/s10052-015-3622-3, arXiv:1506.08008 [hep-ph].

[42] M. Buschmann, C. Englert, D. Goncalves, T. Plehn, M. Spannowsky, Phys. Rev. D 90 (1) (2014) 013010, http://dx.doi.org/10.1103/PhysRevD.90.013010, arXiv:1405.7651 [hep-ph].

[43] S. Taheri Monfared, S. Fayazbakhsh, M. Mohammadi Najafabadi, Phys. Lett. B 762 (2016) 301, http://dx.doi.org/10.1016/j.physletb.2016.09.055, arXiv:1610.02883 [hep-ph].

[44] S. Banerjee, T. Mandal, B. Mellado, B. Mukhopadhyaya, J. High Energy Phys. 1509 (2015) 057, http://dx.doi.org/10.1007/JHEP09(2015)057, arXiv:1505.00226 [hep-ph].

[45] S. Kumar, P. Poulose, S. Sahoo, Phys. Rev. D 91 (7) (2015) 073016, http://dx.doi.org/10.1103/PhysRevD.91.073016, arXiv:1501.03283 [hep-ph].

[46] F. Maltoni, E. Vryonidou, C. Zhang, J. High Energy Phys. 1610 (2016) 123, http://dx.doi.org/10.1007/JHEP10(2016)123, arXiv:1607.05330 [hep-ph].

[47] R.M. Godbole, D.J. Miller, K.A. Mohan, C.D. White, J. High Energy Phys. 1504 (2015) 103, http://dx.doi.org/10.1007/JHEP04(2015)103, arXiv:1409.5449 [hep-ph].

[48] E. Boos, V. Bunichev, M. Dubinin, Y. Kurihara, Phys. Rev. D 89 (2014) 035001, http://dx.doi.org/10.1103/PhysRevD.89.035001, arXiv:1309.5410 [hep-ph].

[49] M.B. Einhorn, J. Wudka, Nucl. Phys. B 877 (2013) 792, http://dx.doi.org/10.1016/j.nuclphysb.2013.11.004, arXiv:1308.2255 [hep-ph].

[50] G. Isidori, M. Trott, J. High Energy Phys. 1402 (2014) 082, http://dx.doi.org/10.1007/JHEP02(2014)082, arXiv:1307.4051 [hep-ph].

[51] S. Khatibi, M. Mohammadi Najafabadi, Phys. Rev. D 90 (7) (2014) 074014, http://dx.doi.org/10.1103/PhysRevD.90.074014, arXiv:1409.6553 [hep-ph].

[52] A. Kobakhidze, N. Liu, L. Wu, J. Yue, Phys. Rev. D 95 (1) (2017) 015016, http://dx.doi.org/10.1103/PhysRevD.95.015016, arXiv:1610.06676 [hep-ph].

[53] H. Khanpour, M. Mohammadi Najafabadi, arXiv:1702.00951 [hep-ph].

[54] D. de Florian, et al., LHC Higgs Cross Section Working Group, arXiv:1610.07922 [hep-ph].

[55] E. Gabrielli, B. Mele, J. Rathsman, Phys. Rev. D 77 (2008) 015007, http://dx.doi.org/10.1103/PhysRevD.77.015007, arXiv:0707.0797 [hep-ph].

[56] G. Buchalla, O. Cata, C. Krause, Nucl. Phys. B 894 (2015) 602, http://dx.doi.org/10.1016/j.nuclphysb.2015.03.024, arXiv:1412.6356 [hep-ph].

[57] G. Buchalla, O. Cata, A. Celis, C. Krause, Phys. Lett. B 750 (2015) 298, http://dx.doi.org/10.1016/j.physletb.2015.09.027, arXiv:1504.01707 [hep-ph].

[58] R. Contino, M. Ghezzi, C. Grojean, M. Muhlleitner, M. Spira, J. High Energy Phys. 1307 (2013) 035, http://dx.doi.org/10.1007/JHEP07(2013)035, arXiv:1303.3876 [hep-ph].

[59] G.F. Giudice, C. Grojean, A. Pomarol, R. Rattazzi, J. High Energy Phys. 0706 (2007) 045, http://dx.doi.org/10.1088/1126-6708/2007/06/045, arXiv:hep-ph/0703164.

[60] R. Barbieri, A. Pomarol, R. Rattazzi, A. Strumia, Nucl. Phys. B 703 (2004) 127, http://dx.doi.org/10.1016/j.nuclphysb.2004.10.014, arXiv:hep-ph/0405040.

[61] A. Abbasabadi, D. Bowser-Chao, D.A. Dicus, W.W. Repko, Phys. Rev. D 58 (1998) 057301, http://dx.doi.org/10.1103/PhysRevD.58.057301, arXiv:hep-ph/9706335.

[62] J. Alwall, et al., J. High Energy Phys. 1407 (2014) 079, http://dx.doi.org/10.1007/JHEP07(2014)079, arXiv:1405.0301 [hep-ph].

[63] J. Alwall, M. Herquet, F. Maltoni, O. Mattelaer, T. Stelzer, J. High Energy Phys. 1106 (2011) 128, http://dx.doi.org/10.1007/JHEP06(2011)128, arXiv:1106.0522 [hep-ph].

[64] A. Alloul, N.D. Christensen, C. Degrande, C. Duhr, B. Fuks, Comput. Phys. Commun. 185 (2014) 2250, http://dx.doi.org/10.1016/j.cpc.2014.04.012, arXiv:1310.1921 [hep-ph].

[65] C. Degrande, C. Duhr, B. Fuks, D. Grellscheid, O. Mattelaer, T. Reiter, Comput. Phys. Commun. 183 (2012) 1201, http://dx.doi.org/10.1016/j.cpc.2012.01.022, arXiv:1108.2040 [hep-ph].

[66] T. Sjostrand, S. Mrenna, P.Z. Skands, Comput. Phys. Commun. 178 (2008) 852, http://dx.doi.org/10.1016/j.cpc.2008.01.036, arXiv:0710.3820 [hep-ph].

[67] T. Sjostrand, L. Lonnblad, S. Mrenna, P.Z. Skands, arXiv:hep-ph/0308153.

[68] J. de Favereau, et al., DELPHES 3 Collaboration, J. High Energy Phys. 1402 (2014) 057, http://dx.doi.org/10.1007/JHEP02(2014)057, arXiv:1307.6346 [hep-ex].

[69] A. Mertens, J. Phys. Conf. Ser. 608 (1) (2015) 012045, http://dx.doi.org/10.1088/1742-6596/608/1/012045.

[70] R.D. Ball, et al., Nucl. Phys. B 867 (2013) 244, http://dx.doi.org/10.1016/j.nuclphysb.2012.10.003, arXiv:1207.1303 [hep-ph].

[71] K.A. Olive, et al., Particle Data Group Collaboration, Chin. Phys. C 38 (2014) 090001, http://dx.doi.org/10.1088/1674-1137/38/9/090001.

[72] M. Cacciari, G.P. Salam, G. Soyez, J. High Energy Phys. 0804 (2008) 063, http://dx.doi.org/10.1088/1126-6708/2008/04/063, arXiv:0802.1189 [hep-ph].

[73] M. Cacciari, G.P. Salam, G. Soyez, Eur. Phys. J. C 72 (2012) 1896, http://dx.doi.org/10.1140/epjc/s10052-012-1896-2, arXiv:1111.6097 [hep-ph].

[74] S. Chatrchyan, et al., CMS Collaboration, J. Instrum. 8 (2013) P04013, http://dx.doi.org/10.1088/1748-0221/8/04/P04013, arXiv:1211.4462 [hep-ex].

[75] C. Englert, R. Kogler, H. Schulz, M. Spannowsky, Eur. Phys. J. C 76 (7) (2016) 393, http://dx.doi.org/10.1140/epjc/s10052-016-4227-1, arXiv:1511.05170 [hep-ph].

[76] M. Gorbahn, J.M. No, V. Sanz, J. High Energy Phys. 1510 (2015) 036, http://dx.doi.org/10.1007/JHEP10(2015)036, arXiv:1502.07352 [hep-ph].

[77] C. Csaki, M.L. Graesser, G.D. Kribs, Phys. Rev. D 63 (2001) 065002, http://dx.doi.org/10.1103/PhysRevD.63.065002, arXiv:hep-th/0008151.

[78] W.D. Goldberger, B. Grinstein, W. Skiba, Phys. Rev. Lett. 100 (2008) 111802, http://dx.doi.org/10.1103/PhysRevLett.100.111802, arXiv:0708.1463 [hep-ph].

[79] C. Degrande, B. Fuks, K. Mawatari, K. Mimasu, V. Sanz, arXiv:1609.04833 [hep-ph].

[80] P. Agrawal, A. Shivaji, Phys. Lett. B 741 (2015) 111, http://dx.doi.org/10.1016/j.physletb.2014.12.021, arXiv:1409.8059 [hep-ph].

[81] E. Gabrielli, B. Mele, F. Piccinini, R. Pittau, J. High Energy Phys. 1607 (2016) 003, http://dx.doi.org/10.1007/JHEP07(2016)003, arXiv:1601.03635 [hep-ph].